AD_____

Award Number: W81XWH-12-1-0137

TITLE: Computational models of anti-VEGF therapies in prostate cancer

PRINCIPAL INVESTIGATOR: Mac Gabhann, Dr. Feilim

CONTRACTING ORGANIZATION: Johns Hopkins University
Baltimore MD 21218-2680

REPORT DATE: June 2014

TYPE OF REPORT: Annual Report

PREPARED FOR: U.S. Army Medical Research and Materiel Command
Fort Detrick, Maryland 21702-5012

REPORT DOCUMENTATION PAGE

Form Approved
OMB No. 0704-0188

1. REPORT DATE	2. REPORT TYPE	3. DATES COVERED
June 2014	Annual	1 June 2013 – 31 May 2014

4. TITLE AND SUBTITLE
Computational Models of anti-VEGF Therapies in Prostate Cancer

5a. CONTRACT NUMBER

5b. GRANT NUMBER
W81XWH-12-1-0137

5c. PROGRAM ELEMENT NUMBER

6. AUTHOR(S)
Mac Gabhann, Dr. Feilim

E-Mail: feilim@jhu.edu

5d. PROJECT NUMBER

5e. TASK NUMBER

5f. WORK UNIT NUMBER

7. PERFORMING ORGANIZATION NAME(S) AND ADDRESS(ES)
Johns Hopkins University

Baltimore MD 21218-2680

8. PERFORMING ORGANIZATION REPORT NUMBER

9. SPONSORING / MONITORING AGENCY NAME(S) AND ADDRESS(ES)
U.S. Army Medical Research and Materiel Command
Fort Detrick, Maryland 21702-5012

10. SPONSOR/MONITOR'S ACRONYM(S)

11. SPONSOR/MONITOR'S REPORT NUMBER(S)

12. DISTRIBUTION / AVAILABILITY STATEMENT
Approved for Public Release; Distribution Unlimited

13. SUPPLEMENTARY NOTES

14. ABSTRACT

The vascular endothelial growth factor (VEGF) family of cytokines promotes vascularization, tumorigenesis and metastasis in many cancers. Our goal is to develop computational models that combine mechanistic topological data on the VEGF protein interaction network with gene expression datasets for a large population of prostate cancers. We have assembled databases of prostate cancer gene expression data, and analyzed the data using bioinformatic techniques, identifying key VEGF-based subgroups of prostate cancer plus biomarkers that identify these groups. This year, we have submitted and revised a manuscript based on this analysis, we expect it to be accepted soon.

We have also created new computational models to simulate prostate cancer, based on the individualized gene expression data. We have used these models to simulate therapies that target the VEGF pathway, including anti-ligands such as bevacizumab and anti-receptors. Among are predictions are estimates of the high degree of variability in response to drugs that is predicted by the model, which is reflected in the results of clinical trials targeting VEGF in prostate cancer.

This progress will continue into Year 3, where we will expand the VEGF family members included in our models, and extract key biomarkers indicative of likely success of VEGF- or VEGFR-targeting therapies.

15. SUBJECT TERMS
Computational Modeling; Personalized Medicine; Therapeutics; Angiogenesis

16. SECURITY CLASSIFICATION OF:			17. LIMITATION OF ABSTRACT	18. NUMBER OF PAGES	19a. NAME OF RESPONSIBLE PERSON
a. REPORT	b. ABSTRACT	c. THIS PAGE			19b. TELEPHONE NUMBER *(include area code)*
U	U	U	UU	17	USAMRMC

Table of Contents

Introduction

The vascular endothelial growth factor (VEGF) family of cytokines promotes vascularization, tumorigenesis and metastasis in many cancers (*1*). Although prostate cancer is vasculature- and VEGF-dependent, Phase III clinical trials have failed to show benefit for the anti-VEGF bevacizumab (*2*). Some recent Phase II clinical trials for castration-resistant prostate cancer have revived hope in this treatment (*3, 4*) and underscored the need to better understand these drugs and their targets. In order to improve our understanding, we will create prostate-cancer-specific computational models of VEGF and its receptors. These models will be used to simulate therapies that target the pathway. The therapies to be tested include anti-ligands such as bevacizumab but also anti-receptors and small molecules such as tyrosine kinase inhibitors (*5*). In this way, we can build on both the successes and the failures of anti-VEGF trials to date in order to develop more effective therapies for prostate cancer.

Body

In this section, we will go through the five tasks outlined in the statement of work and describe the progress made towards accomplishing these tasks.

Task 1. Collate the publicly available prostate cancer gene expression datasets. (months 1-36)
1a. Collate the currently available datasets (months 1-3)
1b. Develop a monitoring policy for new datasets and (months 1-3)
1c. Incorporate new datasets as they become available (months 4-36)

Progress to date for Task 1: We have identified the publicly available datasets for prostate cancer gene expression, and we have assembled these into working databases for our needs. Because these high-throughput studies use different platforms, we keep those separate and only perform comparative analyses on datasets with the same platform. For example, we do not mix RNASeq datasets with microarray datasets. However, we do compare the outcomes of these analyses, to determine whether there the qualitative insights are consistent from set to set. An example of this methodology is available in our published breast cancer study (*6*), and in our prostate cancer study currently under review. For that study, we work with hundreds of primary tumor samples from the TCGA study, quantified using RNASeq, and with many additional primary and metastatic tumor samples from other microarray-based datasets. As defined in the statement of work, we will continue to collect and analyze datasets as the project progresses.

Task 2. Analyze the gene expression datasets (months 1-12)
2a. Bioinformatic analysis of angiogenesis genes for prostate cancer (months 1-9)
2b. Write manuscript describing findings (months 9-12)

Progress to date for Task 2: We have analyzed the collated prostate cancer data, written a manuscript based on this, submitted it for review and completed revisions.

There are clear differences between the regulation of VEGF family members in prostate tumors, compared to that in other tumor types (**Fig. 1**). In particular, several members of the VEGF family are downregulated in primary prostate tumors. However, VEGF/Semaphorin biomarkers could be identified that correlated with biochemical recurrence (**Fig. 2**) and metastasis (**Fig. 3**). We investigated the differences between intra-individual variation and inter-individual variation (**Fig. 4**) and used computational models to estimate which of the individual prostate tumors would be expected to be more or less susceptible to anti-VEGF or pro-Sema treatment (**Fig. 5**). This leads into further analysis that will be discussed as part of Tasks 3 and 4.

A manuscript based on these findings has been submitted.

Task 3. Build canonical prostate cancer VEGF transport model (months 1-15)
3a. Collate anatomical and other prostate-specific parameters (months 1-12)
3b. Build computational model of prostate cancer within human body (months 3-6)
3c. Simulate and analyze prostate cancer with representative (average) gene expression (months 6-12)
3d. Write manuscript based on canonical (average) prostate cancer VEGF model (months 12-15)
3e. Post code for model on public model database sites (after manuscript acceptance)

Progress to date for Task 3: We have built and validated the transport model for prostate cancer, and used it to simulate the differences between individuals with specific tumor gene expression characteristics based on actual patient data. The efficacy of drugs that target proteins is dependent on the protein interaction network of the target, and thus we test not just the differences between these individuals at baseline, but also the differences in the responses of these individuals to therapeutic intervention. This is important, because there are several VEGF isoforms and multiple VEGF receptors on endothelial cells (*7*). The overall vascular response to the drug would not be obvious in advance because of the multiple competing ligands and receptors. Only by including all of these in a computational simulation can we find the impact of the drug, and how that impact changes depending on the variable expression of the competing ligands and receptors.

Task 4. Build virtual patient bank (months 12-36)
4a. Incorporate available patient-specific parameters into computational models (months 12-18)
4b. Monitor new datasets (see #1c above) and add virtual patients as appropriate (months 18-36)

Progress on Task 4: We used the model developed in Task 3 to predict the impact of VEGF and Sema changes on the activation on VEGF receptors in normal, primary, and metastatic cancer (**Fig. 5**). The prediction is that there is high variability in the level of activation of both Plexins and VEGFRs. Thus, distinct populations of tumors can be identified that would be expected to be vulnerable or invulnerable to inhibition of VEGF-VEGFR2 or to upregulation of Sema-Plexin.

We have also simulated the transport and receptor binding of VEGFA in compartmental models representing a *population* of prostate cancer patients. The simulation results show multiple different metrics that the model can output to relate to angiogenesis signaling. Each dot on the graphs represents a different individual's tumor. **Fig. 5** shows the effect of each of 4 gene expression inputs on various simulated model features. VEGFA expression (left column) has the strongest association with the features related to VEGF concentrations and receptor binding. Surprisingly, the correlations between VEGFA expression and total VEGFR1/VEGFR2 binding are higher than the correlations between VEGFA expression and plasma total VEGF/tumor free VEGF. This kind of insight is very relevant when it comes to assessing plasma VEGF as a potential biomarker for diagnosis, prognosis, and evaluation of treatment response.

Task 5. Test anti-VEGF pathway therapies against the virtual patient population (months 18-36)
5a. Incorporate anti-VEGF pathway therapies into the canonical code (months 18-21)
5b. Test the anti-VEGF pathway therapies against the population of virtual patient models (months 21-36)
5c. Analyze the data from these results, in particular a bioinfomatic analysis to reduce the number of possible therapies and identify contiguous therapy-responsive subgroups of patients with accompanying biomarkers (months 21-36)
5d. Write manuscript based on virtual patient-specific predictions (months 33-36)
5e. Post code for model on public model database sites (after manuscript acceptance)

Progress on Task 5: We have taken the patient-specific models of Task 4 even further and used them to simulate anti-VEGF therapies, including an anti-VEGF antibody (**Fig. 6**), and an anti-NRP antibody (**Fig. 7**). The impact of these antibodies shows that therapies induce very different changes in the activation of key VEGF receptors, depending on the specific individual. Some individuals would see a large decrease in VEGF signaling, some would see only a small decrease, and a small number will even see a counterintuitive increase (see, for example, samples with a positive fold change in VEGFR2 binding). We can use this data to create a heat map (**Fig. 8**) which shows the relative ability of the two tested therapeutics to positively impact the tumor. While in Figs. 6&7, it appears that VEGF gene expression is the primary driver of the size of the response, our

investigation shows that this is an artifact of an assumption that gene expression variability between tumors was solely due to variability on the tumor cells themselves (i.e. that endothelial cells were the same in each individual). This is increasingly being shown to not be the case, because the tumor cells influence gene expression on the endothelial cells as well. When we include endothelial expression variability (**Figs. 9&10**) we see that the variability increases significantly and the dependence on VEGF is significantly reduced.

Key Research Accomplishments

- Submission of manuscript describing our prostate cancer analysis of VEGF family expression
- Development of prostate-specific computational model of VEGF transport
- Simulation of patient-specific computational models, before and after therapy with anti-VEGF and anti-NRP1
- Analysis of the predicted variability in response to therapeutics across the prostate cancer population.
- Identification of possible biomarkers for success of therapeutics in prostate cancer

Reportable Outcomes

I have presented components of this work at three invited oral presentations:

F. Mac Gabhann. Population Pharmacodynamics: Mechanism-based Modeling of the Angiogenesis Receptor Kinome in Cancer. *Targeting VEGF-mediated Tumor Angiogenesis in Cancer Therapy* (NYAS, New York, NY, June 2014)

F. Mac Gabhann. Computational and Experimental Studies of Growth Factor-Receptor Networks. *Lafayette College* (Lafayette, PA, November 2013)

F. Mac Gabhann. Computational Design of Therapeutics to Target Receptor Tyrosine Kinase Networks. *PLoS Comp Biol Editors' Meeting* (Washington, DC, October 2013)

Publications:

R.J. Bender & F. Mac Gabhann. Dysregulation of the Vascular Endothelial Growth Factor and Semaphorin ligand-receptor families in prostate cancer metastasis (in review) [Figures 1-5 come from this paper; 15 additional/supplementary figures have been omitted]

R.J. Bender & F. Mac Gabhann. Prediction of patient-specific prostate cancer therapeutics by simulating receptor tyrosine kinase networks (in preparation) [Figures 6-10 come from this manuscript]

We have also been invited to contribute a review of this work for an upcoming special issue of the *Annals of the New York Academy of Sciences*

Conclusion

As described above, we have collated prostate cancer gene expression data, analyzed the data using bioinformatic techniques, and created new computational models to simulate prostate cancer, based on the individualized gene expression data. We have tested multiple anti-VEGF therapies in the model, and identified a possible source in the large interindividual variability in response to anti-VEGF therapies.

So what: Without the computational model, the extensive knowledge of mechanisms that have resulted from many researchers studying these pathways could not be used in combination with the high-throughput data. In short, our models allow us to place the individualized data in its correct context – the complex molecular interaction networks inside tumors.

References

1. C. Kut, F. Mac Gabhann, A. S. Popel, Where is VEGF in the body? A meta-analysis of VEGF distribution in cancer. *Br J Cancer* **97**, 978 (Oct 8, 2007).
2. Y. Wu, J. E. Rosenberg, M. E. Taplin, Novel agents and new therapeutics in castration-resistant prostate cancer. *Current opinion in oncology* **23**, 290 (May, 2011).
3. Y. M. Ning *et al.*, Phase II trial of bevacizumab, thalidomide, docetaxel, and prednisone in patients with metastatic castration-resistant prostate cancer. *J Clin Oncol* **28**, 2070 (Apr 20, 2011).
4. J. Picus *et al.*, A phase 2 study of estramustine, docetaxel, and bevacizumab in men with castrate-resistant prostate cancer: results from Cancer and Leukemia Group B Study 90006. *Cancer* **117**, 526 (Feb 1, 2011).
5. J. B. Aragon-Ching, W. L. Dahut, VEGF inhibitors and prostate cancer therapy. *Current molecular pharmacology* **2**, 161 (Jun, 2009).
6. R. J. Bender, F. Mac Gabhann, Expression of VEGF and semaphorin genes define subgroups of triple negative breast cancer. *PLoS One* **8**, e61788 (2013).
7. F. Mac Gabhann, A. S. Popel, Systems biology of vascular endothelial growth factors. *Microcirculation* **15**, 715 (Nov, 2008).

Appendices

None

Supporting Data

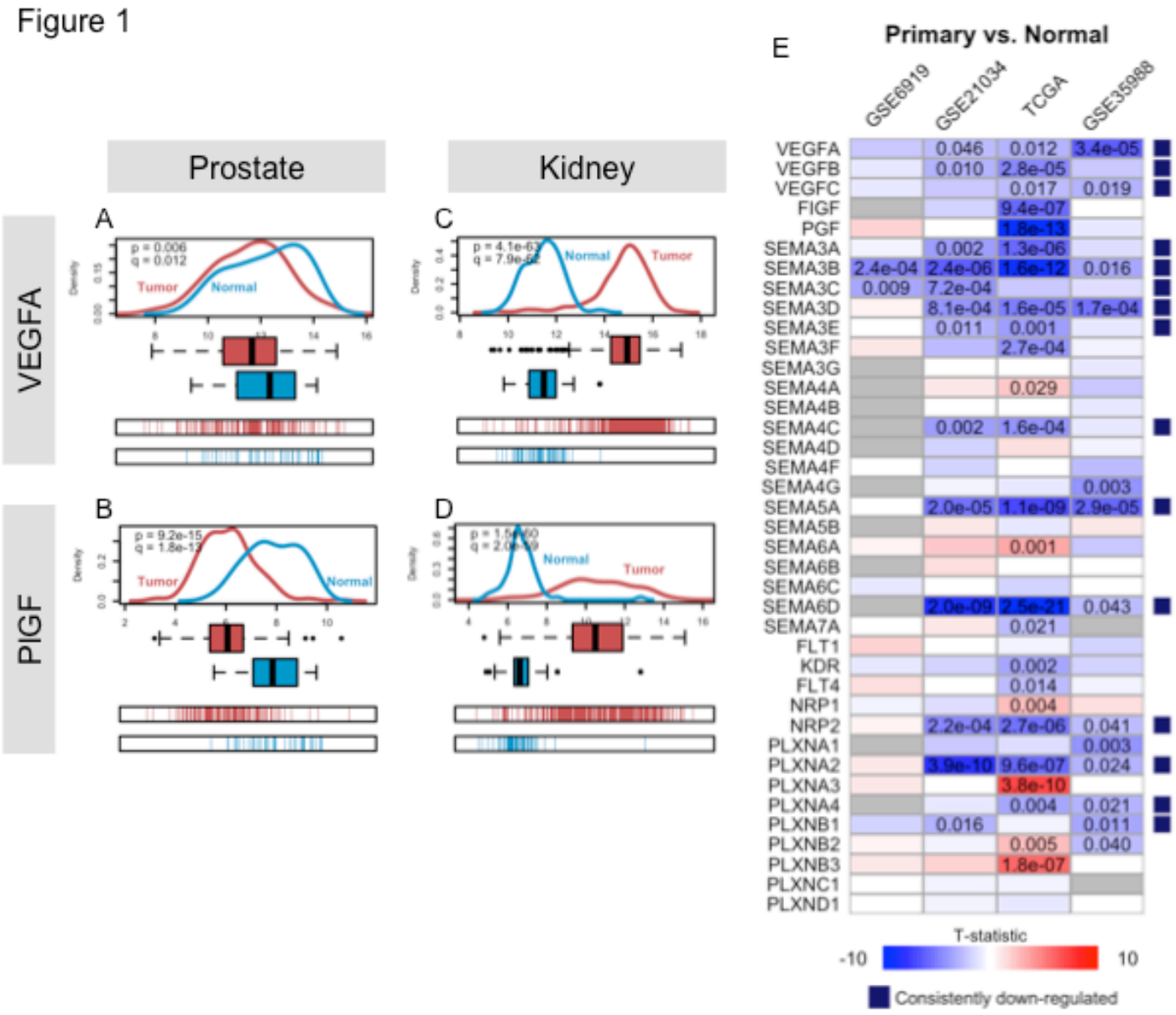

Figure 1: Down-regulation of pro- and anti-angiogenic ligands in primary prostate tumors. A-B: *VEGFA* (A) and *PGF* (B) are expressed less in prostate tumors than in normal prostate tissue in the TCGA dataset, as shown by the density plots (top), box plots (middle), and spike plots (bottom). **C-D:** This contrasts with the TCGA renal cell carcinoma (kidney) dataset, where *VEGFA* (C) and *PGF* (D) are heavily up-regulated in tumors. **E,** *VEGFA* down-regulation is observed across TCGA and microarray datasets, as well as consistent down-regulation of class 3 semaphorins. The number in the boxes indicates the two-tailed *t*-test p-value after multiple testing correction with the Benjamini-Hochberg procedure. Only comparisons with corrected p-values less than 0.05 are displayed. The colors of the boxes indicate the magnitude of the *t*-statistic. The blue boxes to the right of the rows indicate that a gene is significantly down-regulated in two or more datasets with no conflicting signs in the significant alterations (i.e. all up- or all down-regulated).

Figure 2

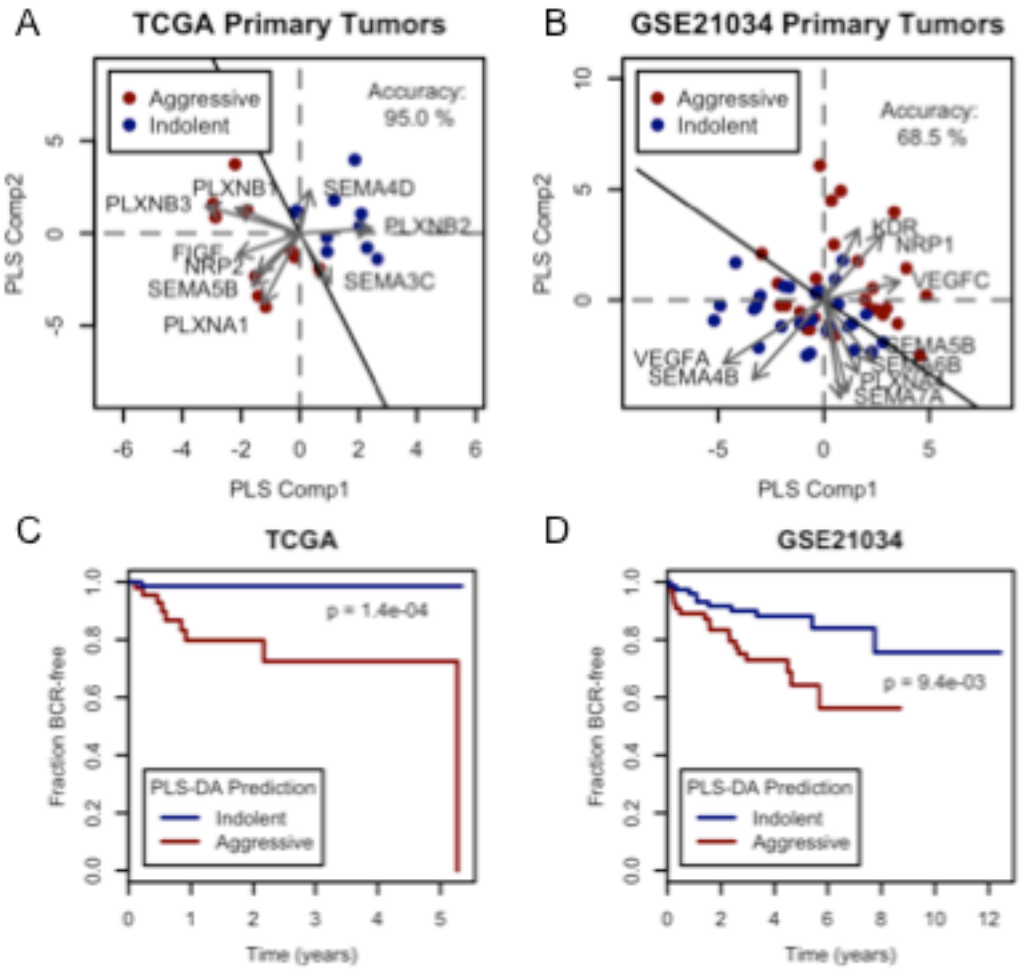

Figure 2: VEGF/Sema expression signatures predicting biochemical recurrence (BCR). A-B: PLS-DA scores/loadings plots for the TCGA (A) and GSE21034 (B) datasets. The training accuracies and the discriminant line separating the two classes are displayed **C-D:** Survival curves show prognostic significance of VEGF/Sema signatures in the TCGA (C) and GSE21034 (D) datasets. The p-values are from log rank tests of the Kaplan-Meier survival estimators for each group.

Figure 3

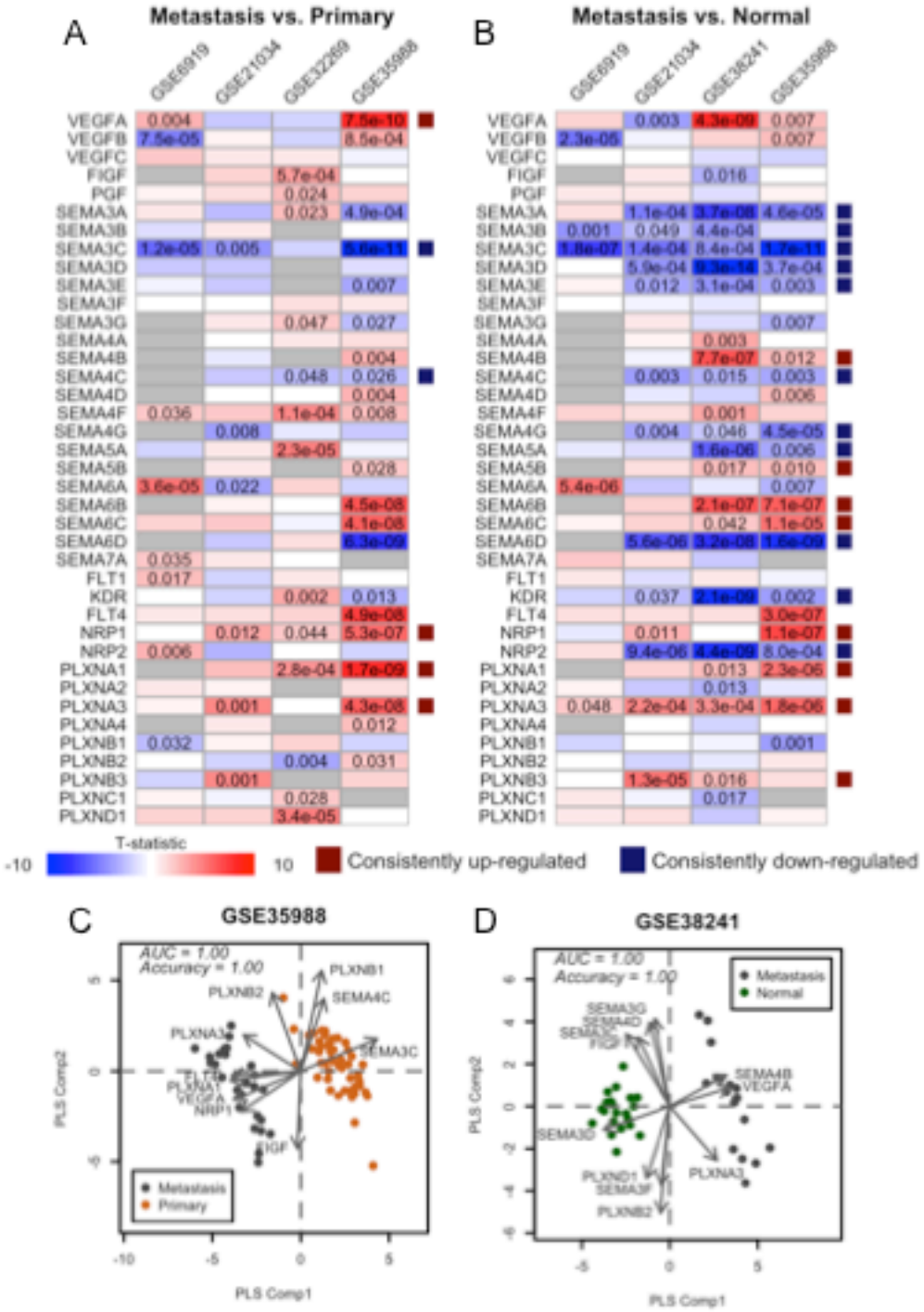

Figure 3: Pro-angiogenic VEGF/Sema gene expression in prostate cancer metastasis. A-B: A greater number of VEGF/Sema genes have recurrent expression alterations when comparing metastases to normal samples (B) than to primary tumor samples (A). The p-values are displayed according to the same criteria as in Figure 1, and red and blue boxes indicate recurrent up- and down-regulation, respectively. **C-D:** PLS-DA scores plots show separation of metastases and primary tumors in GSE35988 (C) and of metastases and normal tissues in GSE38241 (D). Each dot represents a sample with colors as indicated. Arrows correspond to gene loadings in the PLS-DA models, with the names of the genes displayed in the vicinity of the arrowhead. Only the genes with the largest magnitude loadings vectors are displayed. Accuracy refers to the accuracy of the LOOCV predictions; AUC refers to the area under the curve of the LOOCV ROC curve. In both cases, values of 1 indicate perfect prediction.

Figure 4

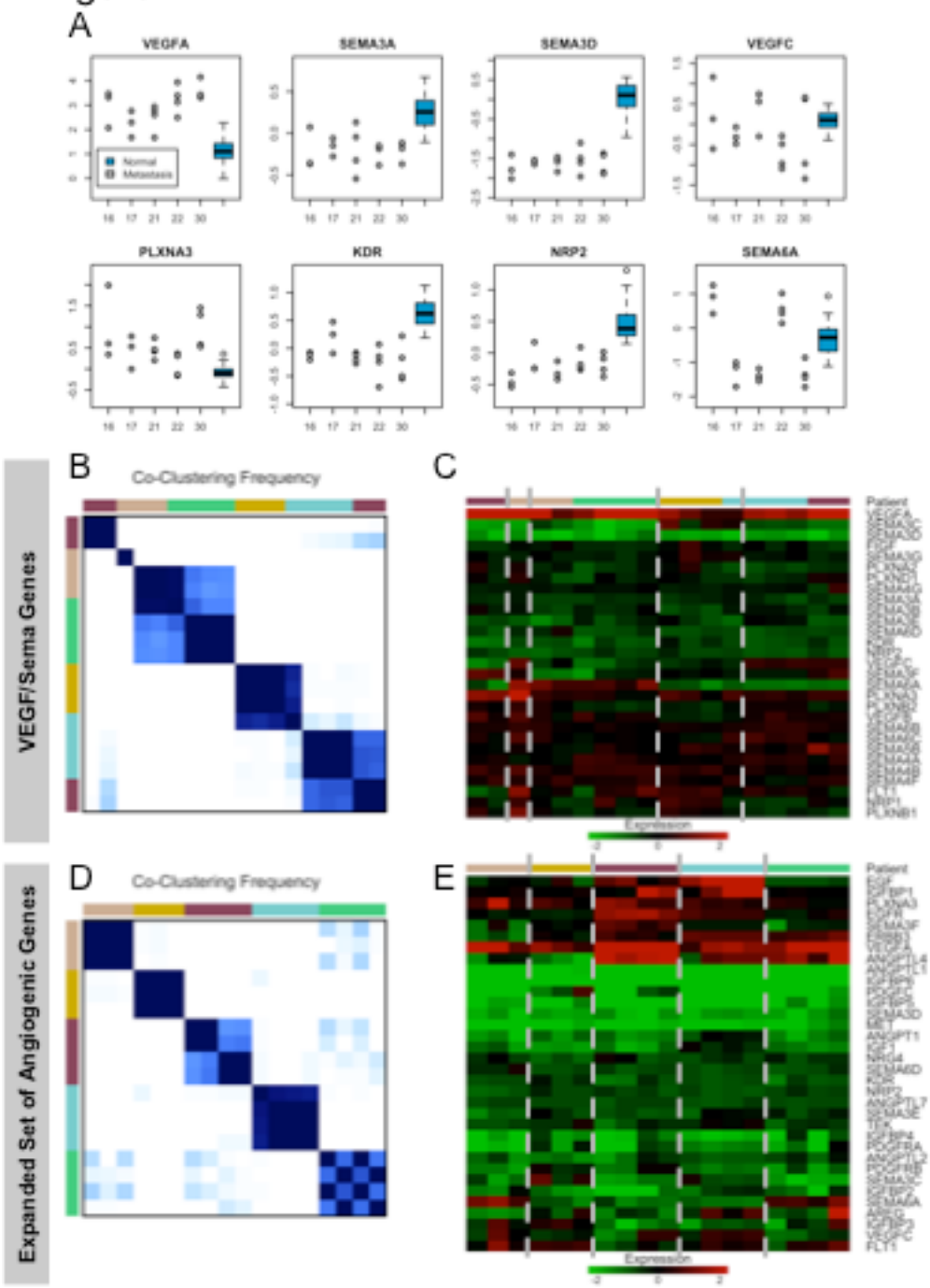

Figure 4: Intra-patient variability of metastases is low relative to inter-patient variability. A: Many genes have consistent alterations in metastatic samples from the same patient while variable expression patterns between patients are more common. Blue box plots indicate the range of expression in the 21 normal samples, with the upper and lower ends of the boxes corresponding to the third and first quartiles of the data, respectively. The numbers along the *x*-axis indicate to which patient the dots above correspond. **B:** Consensus *K*-means clustering of GSE38241 metastases according to VEGF/Sema expression shows a consistent co-clustering pattern for 5 clusters. Dark blue indicates a high frequency of co-clustering between consensus runs, while white indicates no co-clustering. Colors at the top and left indicate the patient from which each metastatic sample was taken. **C:** Heatmap of gene expression across 18 GSE38241 metastases. The mean expression of each gene in the normal prostate tissue samples is subtracted from the expression of each gene in the metastases so that the heatmap shows up/downregulation relative to normal. Only the most variable of the VEGF/Sema genes are displayed. Dashed lines separate clusters, and colors at the top correspond to patients as in B. **D-E:** As for B and C, but with the set of 85 angiogenesis-related genes.

Figure 5

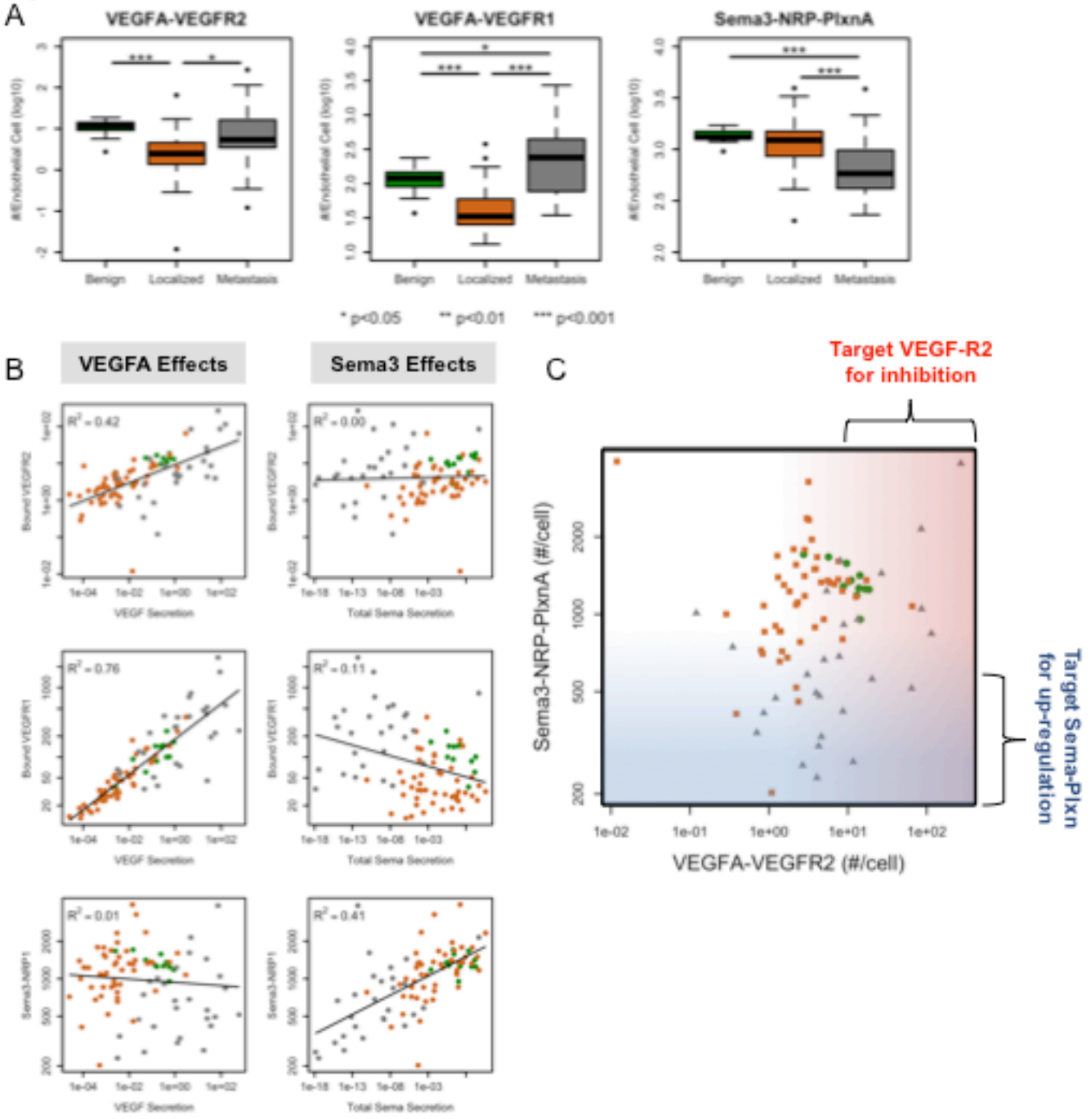

Figure 5: Simulated VEGF/Sema ligand-receptor binding on endothelial cells. A: VEGFR2 (left), VEGFR1 (middle), and Sema3-NRP1 (right) binding in benign prostate (n=12), primary tumors (n=49) and metastatic tumors (n=27) in the GSE35988 dataset. **B:** VEGF secretion and total Sema3 secretion most strongly affect their respective ligand-receptor complexes although weak competitive effects are observed. Lines represent least squares fits of the log-transformed simulated receptor binding data to the gene expression data. R^2 values represent the proportion of variance explained by the least squares fit. **C:** Scatter plots of simulated VEGFA-VEGFR2 and Sema3-NRP-PlxnA across tissue types show that only a subset of metastatic samples fall into the expected anti-VEGFA responsive category, i.e. high VEGFA-VEGFR2 signaling and low Sema3-NRP-PlxnA signaling. Gradients correlate with expected favorability for angiogenesis: darker red for higher VEGFA-VEGFR2 and darker blue for lower Sema3-NRP-PlxnA. Point colors indicate tissue type and are the same as in (A) and (B).

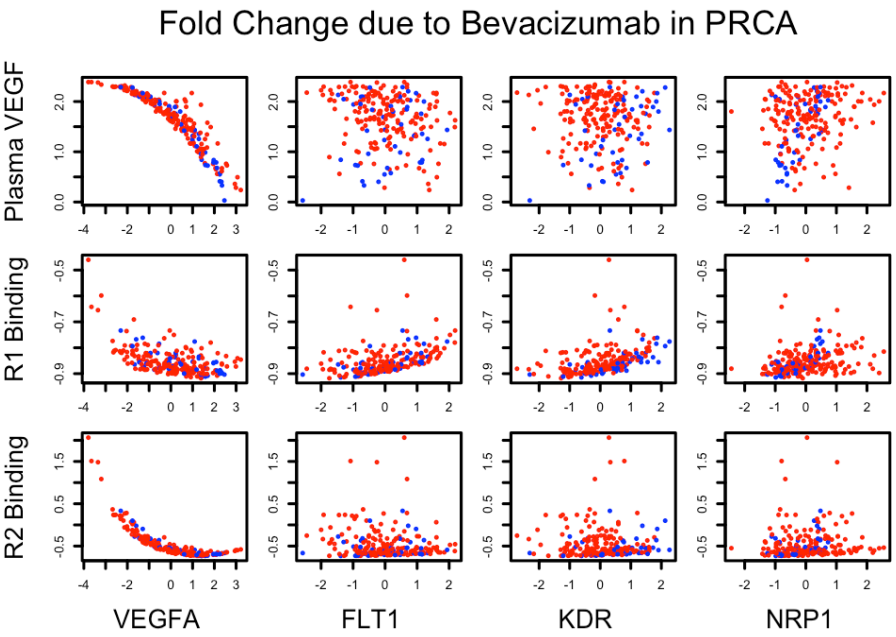

Figure 6. Impact on plasma VEGF, and binding of endothelial VEGFR1 and VEGFR2, of anti-VEGF antibody. This is a population of individualized prostate cancer whole-body multicompartment PK/PD models. Each dot represents one individual from the TCGA PrCa dataset. Red = tumor; blue = normal. The same data is plotted in each column, sorted using the expression of the gene indicated on the x-axis; predicted variables are plotted on the y-axis as fold changes from baseline, and are different in each row.

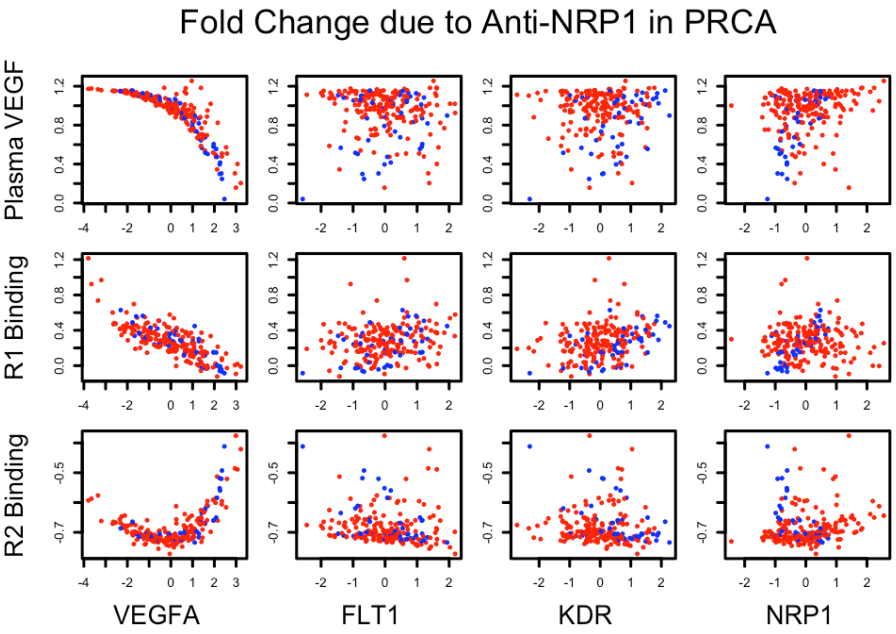

Figure 7. Impact on plasma VEGF, and binding of endothelial VEGFR1 and VEGFR2, of anti-NRP1 antibody. This is a population of individualized prostate cancer whole-body multicompartment PK/PD models. Each dot represents one individual from the TCGA PrCa dataset. Red = tumor; blue = normal. The same data is plotted in each column, sorted using the expression of the gene indicated on the x-axis; predicted variables are plotted on the y-axis as fold changes from baseline, and are different in each row.

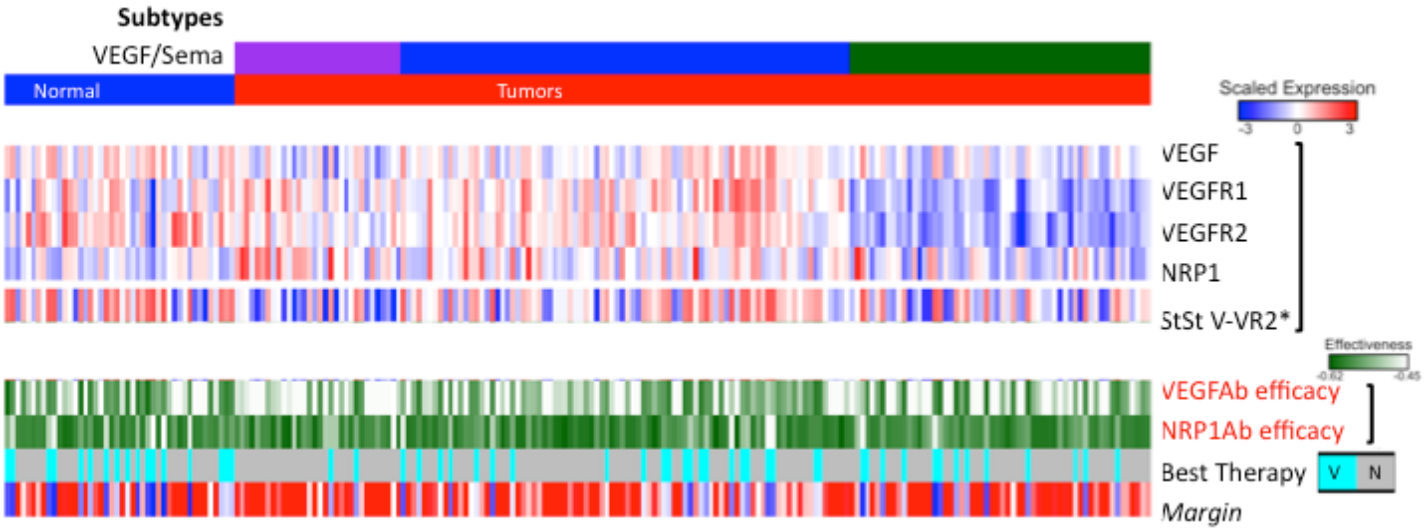

Figure 8. Gene expression and predicted therapeutic efficacy across all the individual tumor samples. Each column is one tumor sample (experimental gene expression data and model predictions). Predicted VEGF/Sema clusters previously identified in prostate cancer are noted at the top, and the 'best choice' therapy is indicated at the bottom.

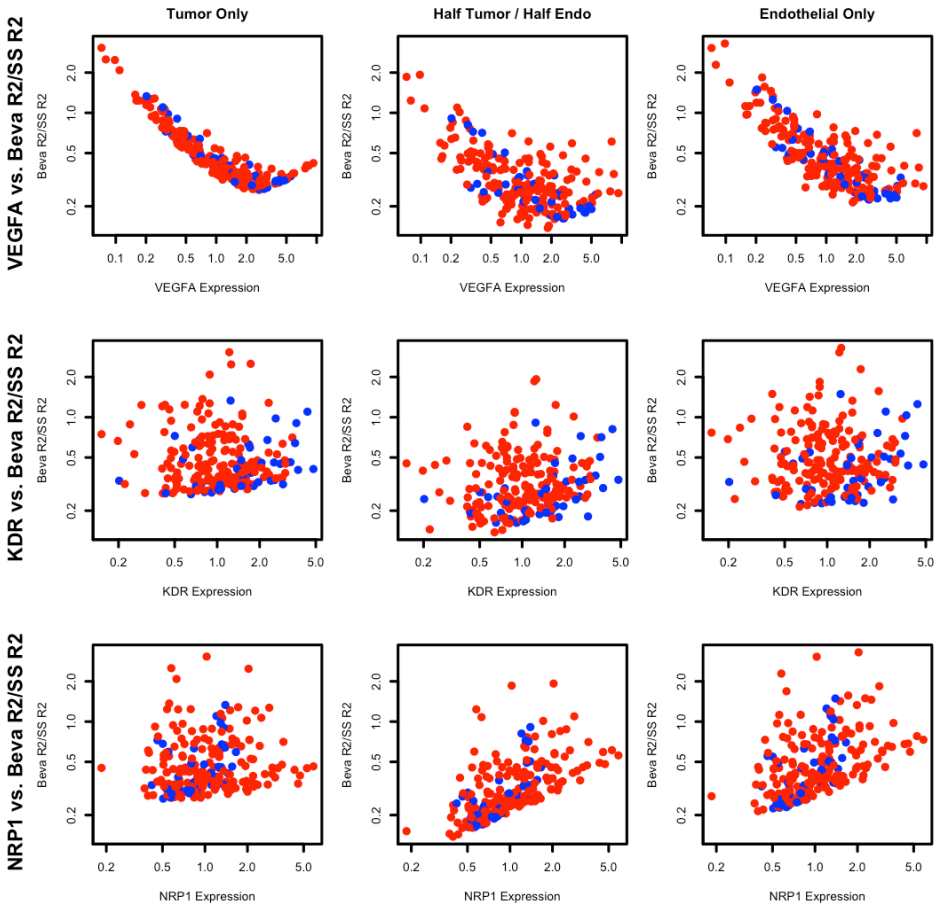

Figure 9. Impact on binding of endothelial VEGFR2 of anti-VEGF antibody depends on the location of gene expression variability. Populations of individualized prostate cancer whole-body multicompartment PK/PD models are plotted in each column, but with differences between the columns of location of gene variability: tumor cells only (left), endothelial cells only (right) or both (middle). Within each column, the results in the three rows are the same, but plotted to show variability in response due to the expression of VEGFA (top), VEGFR2 (middle) and NRP1 (bottom). Each dot represents one individual. Red = tumor; blue = normal.

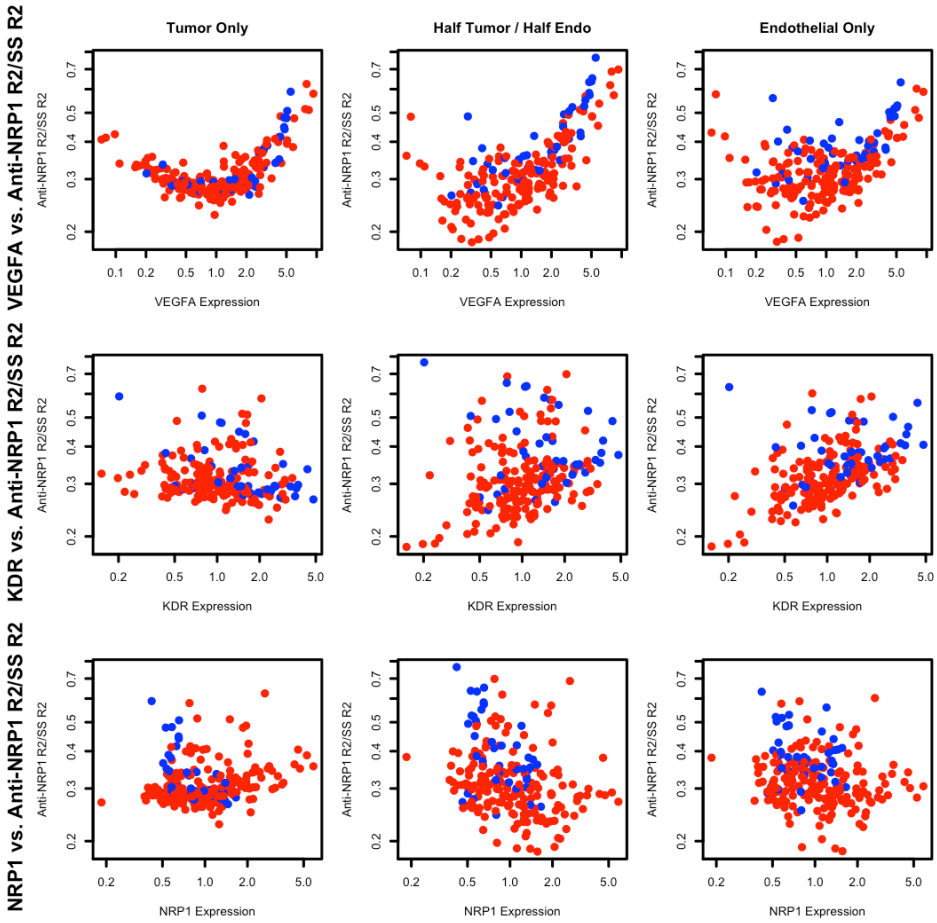

Figure 10. Impact on binding of endothelial VEGFR2 of anti-NRP1 antibody depends on the location of gene expression variability. Populations of individualized prostate cancer whole-body multicompartment PK/PD models are plotted in each column, but with differences between the columns of location of gene variability: tumor cells only (left), endothelial cells only (right) or both (middle). Within each column, the results in the three rows are the same, but plotted to show variability in response due to the expression of VEGFA (top), VEGFR2 (middle) and NRP1 (bottom). Each dot represents one individual. Red = tumor; blue = normal.